



International Conference on the Technology of Plasticity, ICTP 2017, 17-22 September 2017,  
Cambridge, United Kingdom

## Effect of Relief-hole Diameter on Die Elastic Deformation during Cold Precision Forging of Helical Gears

Wei Feng<sup>a</sup>, Jiying Lv<sup>a</sup>, Lin Hua<sup>b,\*</sup>, Hui Long<sup>c</sup>, Feng Wang<sup>a</sup>

<sup>a</sup>*School of Materials Science and Engineering, Wuhan University of Technology, Wuhan 430070, China*

<sup>b</sup>*School of Automotive Engineering, Wuhan University of Technology, Wuhan 430070, China*

<sup>c</sup>*Department of Mechanical Engineering, The University of Sheffield, Sheffield, S1 3JD, UK*

---

### Abstract

During cold precision forging of helical gears, the die experiences high forming pressure resulting in elastic deformation of the die, a main factor affecting dimensional accuracy of a formed gear. The divided flow method in material plastic deformation is an effective way to reduce the forming force and the die pressure during cold precision forging of helical gears. In this study, by utilizing the flow-relief-hole method, a billet design with different initial diameters of the relief-hole is developed to improve the dimensional accuracy of cold forging gears. Three-dimensional Finite Element (FE) models are established to simulate the plastic deformation process of billet during cold precision forging of a helical gear and to determine the forming force acting on the die. Further models of die stress analysis are developed to examine the die elastic deformation and distribution of the displacement. Effects of the relief-hole diameters on die elastic deformation are studied. The results show that the elastic deformation of the die is different in the addendum, dedendum, and involute parts of forging gear using different relief-hole diameters. The die elastic deformation increases firstly and then decreases when the relief-hole diameter increases. The tooth portions are of larger elastic deformation and the peak value locates in the addendum. It shows the importance of optimizing the relief-hole diameter to minimize the dimensional inaccuracy of forging gears caused by the die elastic deformation.

© 2017 The Authors. Published by Elsevier Ltd.

Peer-review under responsibility of the scientific committee of the International Conference on the Technology of Plasticity.

*Keywords:* Cold precision forging; helical gear; relief-hole design; elastic deformation.

---

\* Corresponding author. Tel.: +086-027-87168391; fax: +086-027-87168391.

E-mail address: [hualin@whut.edu.cn](mailto:hualin@whut.edu.cn); [fengwei@whut.edu.cn](mailto:fengwei@whut.edu.cn)

## 1. Introduction

Precision forging process of helical gear has been widely studied in gear manufacturing because of its well-known advantages compared with conventional cutting methods [1-3]. High dimensional accuracy is one of the main objectives in the cold forging of helical gears in order to meet the requirement of its industrial standards. Many factors influence the dimensional accuracy of the forged gear during the cold forging process, such as the material properties of the workpiece and tool, elastic deformation behaviour of the tools/dies and lubricant condition between workpiece and tool. Many recent studies have been carried out to investigate the effect of key factors and evaluation methods of the dimensional accuracy in the forging process. Lee et al. [4][5] investigated the effects of different forging stage on dimensional accuracy of a cold-forged spur gear and evaluated the elastic deformation characteristics of a cold forging tool using experiment and FEM analysis method. Sadeghi et al. [6] studied the fundamental mechanics of dimensional variations of precision forged cylinder in room or elevated temperature by theoretical analysis and experiment method to predict the final forging dimensions. Long and Balendra [7] investigated the combined influence of the elastic characteristics and thermal changes on the dimensional accuracy of back-extrusion of low-carbon steel and pure aluminium components using FE simulation. Yilmaz and Eyercioglu [8] analyzed the influence of elastic die expansion and workpiece contraction on the dimensional variations in a precision forging using theoretical and experimental methods. Hu and Hai [9] designed a special experimental device to measure the pressure distribution on a die surface and studied the influence of different parameters during upsetting. Lu and Ou [10] studied the press elastic behaviour and quantified its effect in the forging of 3D complex shapes using a stiffness matrix formulation, and results showed that the press elasticity influences the dimensional and shape accuracy of the forged part.

Because of the complex shape of helical gear, the forging load is very high, which results in die elastic deformation and affects the forged helical gear dimensional accuracy during the cold forging of helical gears. Therefore, it is necessary to develop a method to reduce the forging load in order to reduce the die elastic deformation. The forging load and die stresses can be reduced effectively using the divided flow method in forging process [11]. In this study, a flow-relief-hole method utilized to design the billet with different initial diameters of the relief-hole to reduce the forging load in cold forging helical gears. Three-dimensional FE models using two steps in the simulation are developed to simulate the plastic deformation process of billet material and die elastic deformation. Effects of different relief-hole diameters on the die elastic deformation are analyzed.

## 2. Establishment of two-step FE models

To analyze the die elastic behaviour, two-step FE models are established. First, a three-dimensional FE model is established to simulate the cold precision forging of a helical gear to determine the forming load acting on the die. The helical gear product formed is right-handed and its specifications of number of teeth, normal module, normal pressure angle, helix angle and teeth width are 17, 2mm, 20°, 20°, 10mm, respectively. Also it is a pitch diameter of 36.18mm and a root diameter of 31.18mm as shown in fig.1(a). Billet with relief-hole is designed to reduce the forging load using the flow-hole-relief principal and the outer diameter of the billet  $D$  is approximately equal to root one of the forged gear in order to save the upsetting time during the forging of a helical gear. In this model, the initial diameter  $d_0$  of the billet is designed to 0, 5, 10, 15, 20mm and the corresponding billet height  $H_0$  is 14.32, 14.73, 16.11, 19.09, 25.77mm according to the law of volume constancy of the material in metal plastic deformation, respectively as shown in fig.1(b). The billet material is 20CrMnTiH, a kind of low-carbon gear steel used widely in China [12]. The billet is defined as a plastic body and all the dies are regarded as rigid ones in FE modelling. The die material is AISI-H13. The number of element of the billet is 300000 after using meshing window and the constant shear friction factor is 0.14 between the dies and the billet. The punch movement speed is 10mm/s. Another model of die stress analysis is developed by defining the final step of the above forging process simulation as the analysis object and applying the forming force obtained in the forging process simulation on the die by interpolating to examine the die elastic deformation and distribution of the displacement. In this model, the die is meshed 400000 elements and defined as an elastic body. The bottom plane of die is Z fixed to prevent die from flying when external force was applied. The two-step FE models are developed as shown in fig. 2.

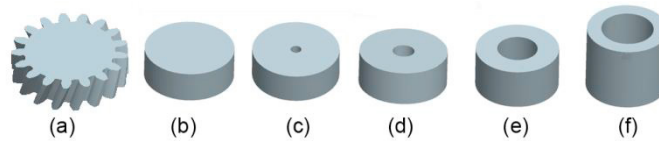


Fig.1.(a) Helical gear formed and billets with relief-hole:(b)  $d_0=0\text{mm}$ , (c) $d_0=5\text{mm}$ , (d)  $d_0=10\text{mm}$ , (e)  $d_0=15\text{mm}$ , (f)  $d_0=20\text{mm}$ .

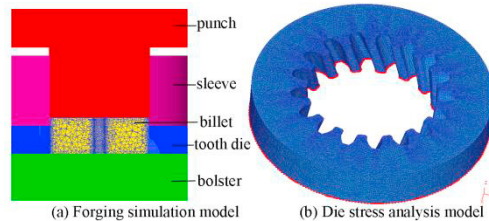


Fig.2. Two-step FE models: (a) forging simulation model; (b) die stress analysis model.

### 3. Results and Discussion

#### 3.1. Forging load under different relief-hole diameters

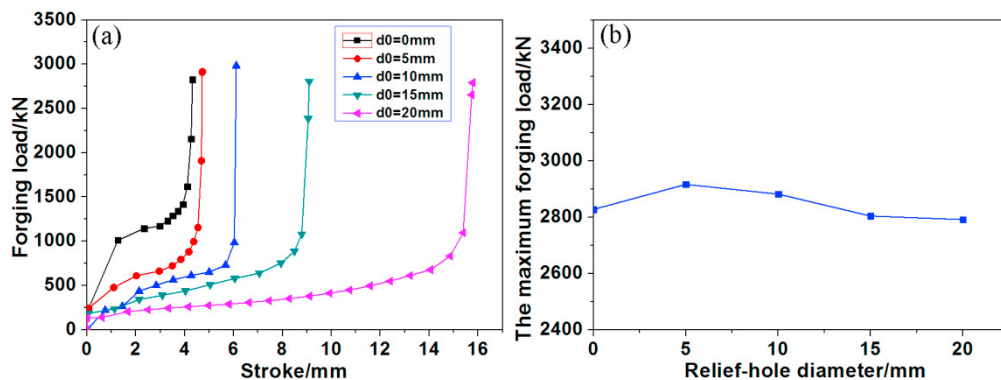


Fig. 3.(a) Load-stroke curve, and (b) the maximum load under different relief-hole diameters.

Fig.3 shows the load-stroke curve and the maximum forging load under different relief-hole diameters. As seen from fig.3(a), the forming load increases gradually with the increasing stroke and the variation trend is much gentler with the increasing the diameter of relief-hole  $d_0$ . The maximum forming load increases first then decreases with the increasing  $d_0$  according to fig.3(b) and the values are 2827, 2916, 2882, 2803, 2791kN at the initial relief-hole diameter of 0, 5, 10, 15, 20mm, respectively. This because the fractional reduction in area of material decreases as the relief-hole diameter increases thus prevents an increase of the forging load through divided flow. And the filling up of the tooth die occurs by combination the inward material flow with the outward material flow during forging.

#### 3.2. Distributions of die stress under different relief-hole diameters

Fig. 4 shows that effective stress distributions and variation of the maximum effective stress of tooth die under different  $d_0$ . From fig. 4(a)-(e) the distribution law is basically the same regardless of the initial relief-hole diameters, that is the circumferential effective stress of the tooth die is more uniform and the maximum stress mainly locates in the root. The maximum die stress increases firstly, and then decreases with increasing  $d_0$  according to fig.4(f), which is correspondence with the variation of forging load.

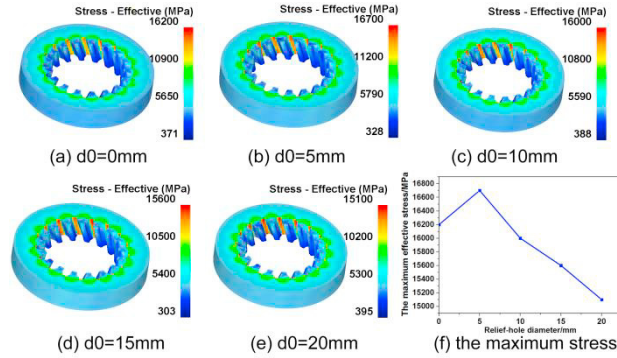


Fig. 4. Distributions of die stress and variation of the maximum effective stress under different  $d_0$ .

3.3. Distributions of elastic deformation under different relief-hole diameters

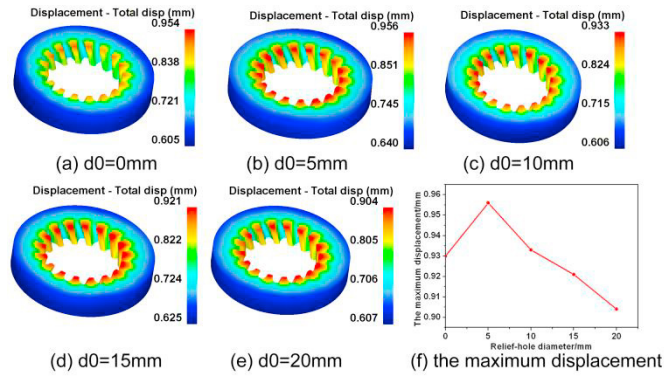


Fig. 5. Distributions of die displacement and variation of the maximum die displacement under different  $d_0$ .

Fig.5(a)-(e) show the distributions of the die displacement which represents the tooth die elastic deformation under different relief-hole diameters  $d_0$ . It is observed that the distribution law is similar under different  $d_0$ . The displacement is uniform circumferentially and is different along tooth width. The tooth portions are of larger elastic deformation and the peak value locates in the addendum under different  $d_0$ . Fig.5 (f) shows the variation of the maximum die displacement under different  $d_0$ . And the amount of the maximum elastic deformation increases firstly, and then decreases with increasing  $d_0$  according to fig. 5(f).

3.4. Elastic deformation characteristics along the tooth width under different relief-hole diameters

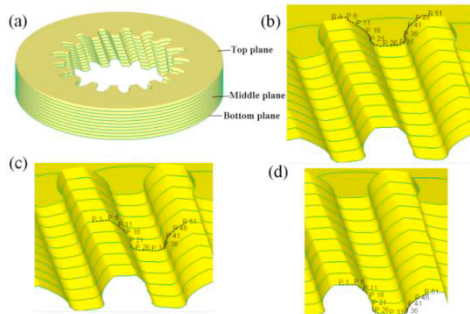


Fig. 6. (a) The contour planes, and tracking points of (b) top plane, (c) middle plane, and (d) bottom plane.

According to the result of the die elastic deformation analysis, the elastic deformation of the tooth die is different along tooth width under different  $d_0$ . To analysis the elastic deformation of the entire tooth die in detail, the tooth die is divided into ten contour planes along the tooth width and three contour planes and one tooth of each contour plane is taken as an example to study on the basis of the rotational symmetry characteristic of tooth die. Some tracking points are set up along the tooth profile curves as the view point to monitor the amount of the displacement to evaluate the elastic deformation behaviour of the tooth die at the three contour planes, as shown in Fig.6.

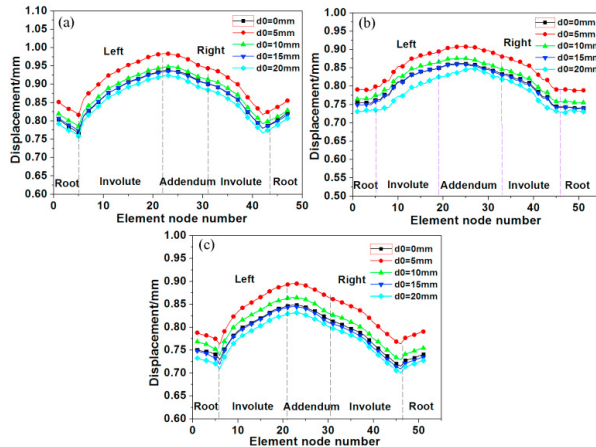


Fig. 7. The elastic deformation characteristics of (a) top plane, (b) middle plane, and (c) bottom plane under different  $d_0$ .

Fig.7 illustrates the elastic deformation characteristics of the three contour planes under different relief-hole diameters. As seen from fig.7, the variation laws of the elastic deformation are the same as the top plane and the bottom plane under different  $d_0$ , but the characteristics of the middle plane are slightly different from the other two planes. The curves all decreased sharply at the transitional position between root and involute under different  $d_0$  and the elastic deformation is different in the addendum, involute and root and the larger values locate in the addendum and the left involute, as can be seen from fig.7(a) and (c). This is because that the forged helical gear is right-hand and is of characteristic of rotational symmetry around the central axis. Also the material flows along the helical profiles and contacts the left side of the tooth firstly and applies the larger normal pressure on the left side. According to fig.7(b), the curves don't decrease sharply at the transitional position between root and involute. The elastic deformation is different in the addendum, involute and root and increases gradually from dedendum to addendum. The larger values locate in the addendum. As can be also seen from fig.7, the elastic deformation increase first, and then decrease with increasing  $d_0$  and the peak values and the minimum are all at  $d_0=5\text{mm}$  and at  $d_0=20\text{mm}$  at the three planes, respectively. The peak value are about 0.983mm, 0.908mm, 0.895mm and the minimum 0.792mm, 0.731mm, 0.680mm at the top plane, middle plane and bottom plane, respectively.

### 3.5. Modification of the tooth die

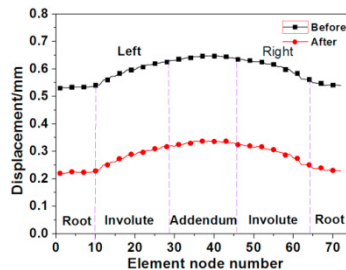


Fig. 8. The elastic deformation characteristics of the forged gear at the middle plane before and after modification under  $d_0=20\text{mm}$ .

Because the shape and dimension of the forged gear are decided by the die, the tooth die should be modified in advance to compensate for the die elastic deformation in order to improve the forged gear accuracy. The amount of

the modification can be obtained in line with the above analysis results and the tooth die profile curve geometry can be corrected using anti-compensation method by 3D CAD software. Next simulation of the forging process and die stress analysis can be carried out again using the modified tooth die. Fig.8 shows the comparison of the amount of elastic deformation of the forged gear at the middle plane before and after modification. It can be observed that the amount of elastic deformation of the forged helical gear is reduced after modification of the die profile curve, which represents that the dimensional accuracy of the forged gear can be improved by reducing the elastic deformation of the tooth die.

#### 4. Conclusions

The billet with different initial diameters of the relief-hole is designed using flow-relief-hole method to reduce the forging load in cold forging helical gears. Three-dimensional and two-step simulation FE models are developed to simulate the plastic deformation process of billet material and die elastic deformation to investigate the effects of the diameters of the relief-hole on elastic deformation characteristics. According to this study, the conclusions can be drawn that the initial relief-hole diameter of the forged billet affects the elastic deformation behaviour during the cold forging helical gears. The die stresses increase firstly then decreases with increasing relief-hole diameter and the maximum stress mainly locates at the dedendum. The distribution of the die elastic deformation is uniform circumferentially and the elastic deformation of the tooth die is different in the addendum, dedendum, and involute parts of the forged gear using different relief-hole diameters. The elastic deformation increases firstly then decreases with increasing the relief-hole diameter. The higher elastic deformation occurs in the tooth portions and the peak value is at the addendum.

#### Acknowledgements

The authors would like to thank the National Natural Science Foundation of China(51475344), Innovative Research Team Development Program of Ministry of Education of China (IRT13087) and EU FP7 Marie Curie Actions: MatProFuture Project (FP7-PEOPLE-2012 IRSES 318968)for the support given to this research.

#### References

- [1] V.Szentmihalyi,K.Lange, Y.Tronel, J.L.Chenot,R.Ducloux, 3-D finite-element simulation of the cold forging of helical gears, *J. Mater. Process. Technol.* 43 (1994) 279–291.
- [2] Y.B.Park, D.Y.Yang, Finite element analysis for precision cold forging of helical gear using recurrent boundary conditions, *Proc. IMechE. Part B: J. Engineering Manufacture*212 (1998) 96–301.
- [3] W.Feng, L.Hua, X.H. Han, Finite element analysis and simulation for cold precision forging of a helical gear, *J. Cent. South Univ.*19 (2012) 3369–3377.
- [4] Y.S. Lee, Y.N. Kwon, J.H. Lee, T. Ishikawa, Experimental and finite element analysis to predict the dimensional changes of a cold-forged spur gear, *Proc. IMechE. Part B: J. Engineering Manufacture*218 (2004) 1051–1057.
- [5] Y.S. Lee, J.H. Lee, J.U.Choi,T. Ishikawa, Experimental and analytical evaluation for elastic deformation behaviors of cold forging tool, *J. Mater. Process. Technol.*127 (2002) 73–82.
- [6]M.H. Sadeghi, T.A. Dean, Analysis of dimensional accuracy of precision forged axisymmetric components, *Proc. IMechE. Part B:J. Engineering Manufacture*205 (1991)171–178.
- [7] H. Long, R.Balendra, Evaluation of elasticity and temperature effects on the dimensional accuracy of back-extruded components using finite element simulation, *J. Mater. Process. Technol.* 80-81 (1998) 665–670.
- [8] N.F.Yilmaz, O.Eyercioğlu, An integrated computer-aided decision support system for die stresses and dimensional accuracy of precision forging dies, *Int. J. Adv. Manuf. Technol.*40 (2009) 875–886.
- [9] X.L.Hu, J.T.Hai, W.M. Chen, Experimental study and numerical simulation of the pressure distribution on the die surface during upsetting, *J. Mater. Process. Technol.*151 (2004) 367–371.
- [10] B. Lu, H.Ou, Quantification of press elasticity in the forging of three-dimensional complex shapes, *Proc. IMechE. Part B: J. Engineering Manufacture*226 (2011) 466–477.
- [11] M. Ogura, K. Kondo, Precision forging of helical gears utilizing divided-flow method, *The seventh Asia Symposium on Precision forging, Guilin, China: JSTP,2000*, pp. 67–70.
- [12] X.H. Han, L.Y. Dong, L.Hua, J. Lan, W.H. Zhuang, Microstructure and texture evolution in cold rotary forging of spur bevel gears of 20CrMnTi alloy. *J. Mater. Eng. Perform.* 25 (2016) 1182–1190.